ACS OMEGA

Open Access

http://pubs.acs.org/journal/acsodf

Article

Study on the Effect of Graphene on Characteristics of Inorganic Polymer Paint

Huyen T. T. Bui, Anh Nguyet Hoang, and Cuong Manh Le*

Cite This: *ACS Omega* 2025, 10, 5503−5516

Read Online

ACCESS | Metrics & More | Article Recommendations

ABSTRACT: This study investigates the effects of graphene on the thermal resistance, corrosion resistance, and surface morphology of inorganic polymer paints. Graphene was incorporated into the paint at concentrations of 0.01, 0.02, 0.05, 0.1, and 0.2% by weight, and its influence was analyzed using a variety of methods, including TGA/DTA thermal analysis, SEM/FESEM imaging, electrochemical impedance spectroscopy (EIS), polarization curve measurements, and FTIR spectroscopy. The findings revealed that the addition of graphene significantly improved the overall performance of the paint. Notably, the optimal graphene concentration of 0.05% increased the heat resistance to 798 °C (5% improvement over the control) and enhanced corrosion resistance by approximately 20% compared to samples without graphene. Furthermore, the graphene-enhanced paint demonstrated smoother surface morphology and improved coating adhesion, with a noticeable reduction in particle porosity and better uniformity, as observed in SEM images. The results also indicate that excessive graphene content (>0.05%) negatively impacts performance due to poor dispersion and surface defects. Importantly, the study confirms the successful integration of graphene into the paint matrix through FTIR spectra and SEM/FESEM analyses, which highlight strong molecular interactions and structural improvements. These findings suggest that graphene, when added in optimal amounts, can significantly enhance the physical and chemical properties of inorganic polymer paints, making it a promising material for applications in high-temperature environments and corrosion protection in industrial and construction fields. Testing adhered to ISO 834-1:2014 standards, ensuring reproducibility and practical relevance.

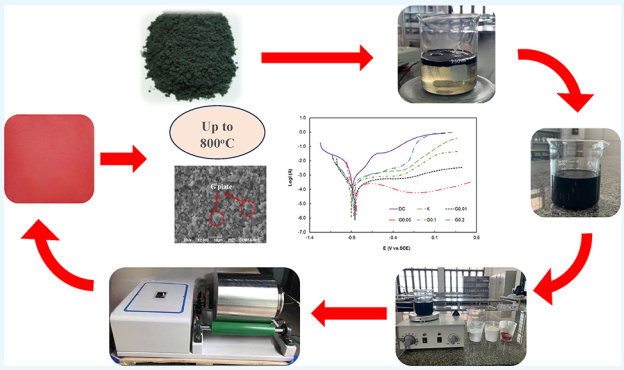

1. INTRODUCTION

Recent advancements in materials science have highlighted the need for high-performance coatings that are both durable and environmentally friendly. Inorganic polymer paints, especially silicate-based systems, have emerged as promising solutions due to their superior thermal stability, corrosion resistance, and environmental compatibility.[1−8] These paints are widely utilized in industries such as construction and infrastructure for protecting steel and concrete surfaces, particularly in high-temperature or corrosive environments.[6,9−16] However, the ongoing development of more advanced coatings is essential to meet the increasing demands for performance and sustainability in industrial applications.

Silicate-based paint, composed of alkali-resistant pigments, fillers, and heat-stable inorganic polymer systems, has garnered considerable attention from scientists and manufacturers alike due to its remarkable properties. Renowned for its antiaging capabilities, silicate paint is a low-toxicity material with minimal or zero emissions of volatile organic compounds (VOCs). It exhibits outstanding resistance to both acidic and alkaline environments, making it highly effective against corrosion. Furthermore, silicate paint is nonflammable, moisture-resistant, and capable of withstanding high temperatures, making it an ideal protective coating for concrete and steel structures.[1,6,10,11,13−16] Despite these advantages, the continuous evolution of science and technology demands further enhancements to meet modern industrial and environmental standards.

Graphene, a revolutionary material composed of a single atomic layer of carbon atoms arranged in a hexagonal lattice, offers unique and unparalleled properties that have sparked significant interest in both fundamental research and practical applications.[17−19] As a nanometer-scale filler, graphene addresses compatibility challenges with organic polymer resins in composite coatings due to its carbon-based structure, which interacts favorably with organic polymers. Studies have

Received: August 29, 2024
Revised: January 13, 2025
Accepted: January 20, 2025
Published: February 4, 2025

https://doi.org/10.1021/acsomega.4c07850
ACS Omega 2025, 10, 5503−5516

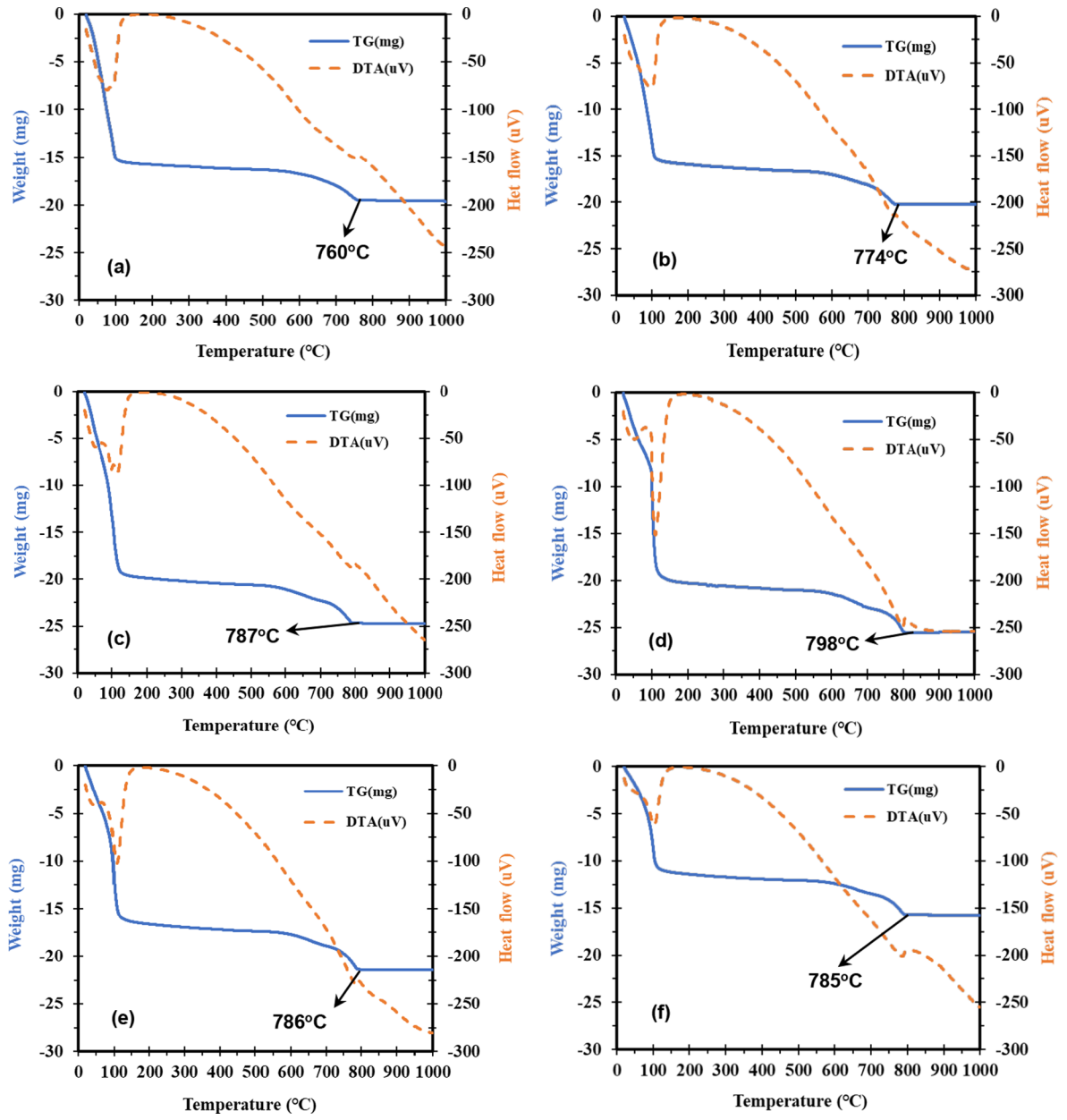

Figure 1. TGA/DTA of K and G paint samples with different Graphene concentrations. (a) Sample K; (b) Sample G-0.0; (c) Sample G-0.02; (d) Sample G-0.05; (e) Sample G-0.1; (f) Sample G-0.2.

demonstrated that incorporating graphene into organic polymer coatings enhances their resistance to corrosion, moisture, and scratches, primarily by improving barrier properties and water contact angles, without compromising curing or adhesion performance.[1−5,20,21]

Although research into integrating graphene into coatings has gained traction, most studies have been limited to composite and organic coatings.[2−5,8,9,11,17,18] The use of graphene in inorganic paints represents a promising frontier, particularly for enhancing the adhesion to metal surfaces. By leveraging graphene's unique molecular structure, graphene-enhanced inorganic paints achieve superior adhesion without requiring labor-intensive surface preparation methods, such as abrasion or chemical treatment. This innovation simplifies the application process, reduces costs, and enhances durability.

The formulation of graphene-enhanced inorganic paints typically involves small graphene concentrations, ranging from 0.001 to 5% by weight, with optimal performance often achieved between 0.1 and 1%. Graphene's presence enables stronger molecular interactions between the paint and metal surfaces, improving adhesion and reducing the need for complex surface treatments. This advanced material not only enhances adhesion but also retains graphene's intrinsic properties, including exceptional corrosion resistance, mechanical strength, and electrical conductivity, making it ideal for industrial and construction applications.

Despite its potential, the influence of graphene on the properties of inorganic polymer coatings remains an emerging research area, with limited studies and applications to date.[11] Our research team has successfully developed high-performance inorganic paints with exceptional heat and corrosion resistance, offering quality comparable to imported products while being cost-effective and environmentally friendly.[19]

https://doi.org/10.1021/acsomega.4c07850
ACS Omega 2025, 10, 5503−5516

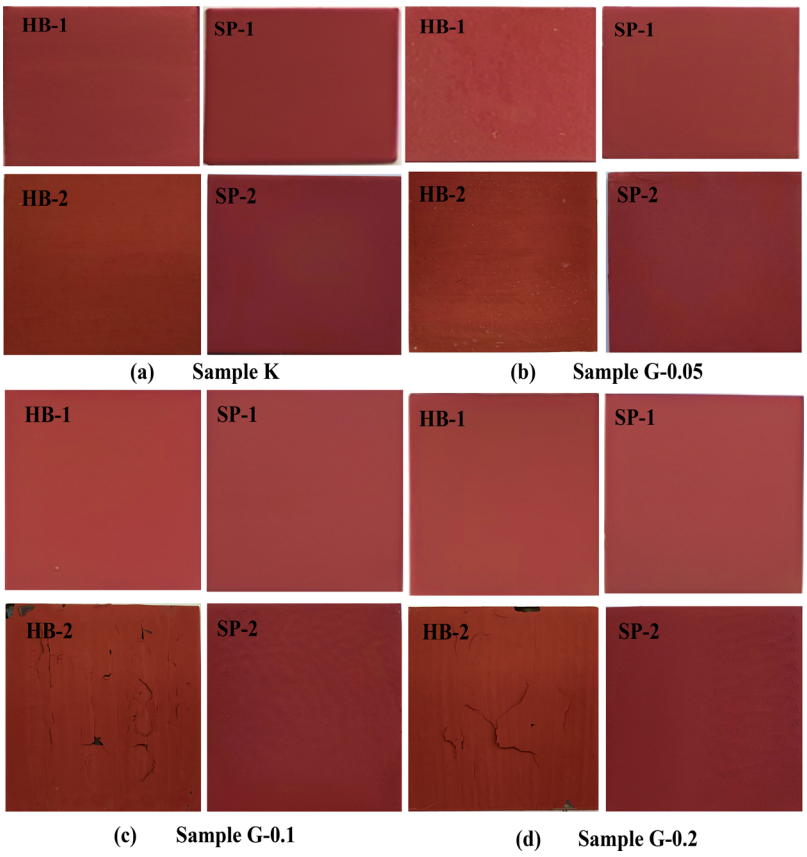

Figure 2. Effect of construction method on heat resistance of paint coating before and after calcination at 650 °C for 1 h. HB: hand brushing; SP: spraying painting; 1: before calcinating and 2: after calcinating.

This study explores the effects of incorporating graphene into inorganic paints at concentrations ranging from 0 to 0.2% by weight. Key properties, including thermal resistance, corrosion resistance, and surface morphology of graphene-enhanced inorganic polymer coatings, were systematically evaluated to offer a comprehensive understanding of this innovative material's potential. The results aim to lay a solid foundation for future developments in graphene-based coatings, addressing both industrial and environmental requirements.

2. RESULTS AND DISCUSSION

2.1. Effect of Graphene on the Heat Resistance of the Paint Coating. *2.1.1. Thermal Analysis Results.* To assess the heat resistance of the paint coating, TGA/DTA thermal analysis methods were conducted for K, G-0.01, G-0.02, G-0.05, G-0.1, and G-0.2 paints. The findings are displayed in Figure 1. The results indicate that sample K can endure temperatures up to 760 °C, while sample G can withstand temperatures ranging from 774 to 798 °C with Graphene concentrations from 0.01 to 0.2%. Notably, the paint sample containing 0.05% G exhibited the highest heat resistance, withstanding temperatures up to 798 °C.

2.1.2. Results of the Firing Method. This study was conducted to evaluate the effects of the calcination temperature, calcination time, and graphene concentration on the heat resistance of paint.

2.1.2.1. Effect of Construction Method on the Heat Resistance of Paint. In this study, paints with different concentrations of Graphene (0, 0.01, 0.02, 0.05, 0.1, and 0.2%) were examined using two different coating methods: hand brushing and spray painting. Steel samples were coated with the paint, allowed to dry naturally, and then subjected to calcination at 650 °C for 1 h. The results are illustrated in Figure 2. A comparison of the painted surface before and after calcination, through visual assessment, reveals a significant influence of the construction method (hand brushing and spray painting) on the steel surface.

Before calcination, the surface of the painted samples that were hand-brushed appeared relatively smooth, but close observation revealed an uneven paint layer thickness. In contrast, the sprayed samples had a flatter, smoother surface compared to that of the hand-brushed ones. After calcination, the surfaces of the hand-brushed samples K and G-0.05 remained smooth, with no signs of peeling. However, when the concentration of G in the paint exceeded 0.05%, the paint surface cracked, peeled, and lost adhesion to the steel substrate. Samples G-0.1 and G-0.2 showed slight blistering. On the other hand, the surfaces of the spray paint samples retained their color after calcination at 650 °C for 1 h. This is attributed to the even coating and good adhesion of the sprayed samples, which performed better after calcination compared to the hand-brushing method.

Furthermore, the influence of graphene concentration on the heat resistance of the paint is evident. As the G concentration exceeds 0.05%, the adhesion and heat resistance of the paint decrease, likely due to poor graphene dispersion in the paint. High Graphene concentrations can cause clustering or surface defects, leading to the observed decrease in performance.

https://doi.org/10.1021/acsomega.4c07850
ACS Omega 2025, 10, 5503−5516

Therefore, the best heat resistance is achieved with a Graphene concentration of 0.05%.

2.1.2.2. Effect of Temperature and Calcination Time on the Heat Resistance of the Paint. The above achievement revealed that the paint still withstands heat well at 650 °C for 1 h; therefore, the samples were calcined at 750 and 800 °C for 2 h to evaluate the influence of calcination temperature and calcination time on the heat resistance of the paint. This assessment was carried out on K paint samples; G-0.05; G-0.1; and G-0.2. The results are presented in Figures 3 and 4.

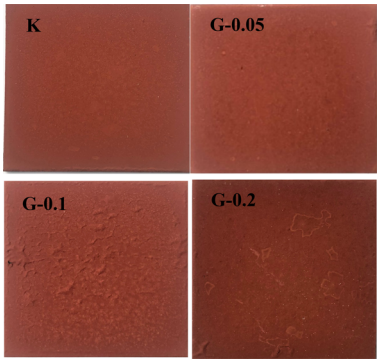

Figure 3. Paint samples after calcinating at 750 °C for 2 h.

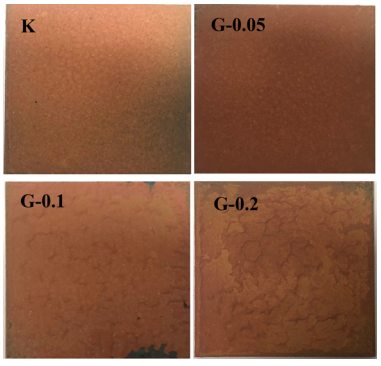

Figure 4. Paint samples after calcinating at 800 °C for 2 h.

After heating at 750 °C for 2 h (Figure 3), the samples changed color (darkened) compared to before heating (as SP-1 sample in Figure 2). However, the surfaces of samples G-0.1 and G-0.2 show signs of slight blistering, but the paint still adheres quite firmly to the substrates.

For the samples after being heated at 800 °C for 2 h (Figure 4), all the surfaces changed to a completely different color and showed more extensive signs of damage than when heated at 750 °C; especially samples G-0.1 and G-0.2 peeling appeared on the edge of the samples. Meanwhile, the paint sample with 0.05% Graphene content was still the best among all samples, the paint layer still adheres well to the steel substrate.

The results after calcination show that the surface of the paint sample with 0.05% Graphene concentration is the best among all the surveyed samples at both 750 and 800 °C. This shows the great influence of graphene concentration in paint on the heat resistance process.

2.1.3. Effect of Graphene on the Heat Shock Resistance of the Paint. The heat resistance in the furnace of the studied paints improved when the paint was added to graphene; the best result was achieved with 0.05 wt % graphene added to the paint. Therefore, the heat shock resistance of the paint surface was carried out with a comparison between the K and G-0.05 paints.

The use of forced heating and direct surface heat pulse testing provided valuable insights into the coatings' thermal resistance under extreme conditions. The controlled heating rates (5 °C/s for forced heating and 10 °C/s for heat pulse) ensured consistency and allowed for the evaluation of temperature gradients across the coating. Notably, the G-0.05 sample exhibited superior resistance, with no visible degradation at peak temperatures of ∼798 °C, while higher graphene concentrations (G-0.1, G-0.2) showed minor blistering and cracking due to agglomeration-induced defects.

Thermal shock torching on painted sample K was performed with 2 samples painted on both sides with 2 torching styles: sample K1 was torched mainly in the middle of the sample, and sample K2 was torched so that the heat was distributed relatively evenly over the entire area of the sample surface. The results (Figure 5) show that, after both K samples were

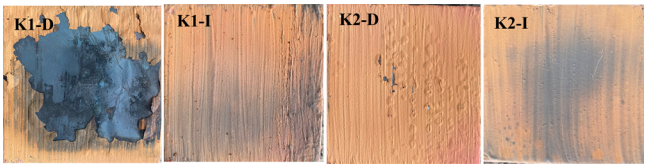

Figure 5. Paint samples K1 and K2 were heated with shock in two different ways: D - Direct side and I - Indirect side.

torched at 650 °C and this temperature was maintained for about 5 min, the surface of the samples had a peeling phenomenon, however, it appeared in 2 samples. Torched differently will be different.

Specifically, for sample K1, the direct torch surface (K1-D) had its paint peeled off; therefore, the paint is no longer able to protect the steel substrate. Although the surface in direct contact with the gas fire was destroyed, the back side (K1-I) of the sample still ensured adhesion and protected the steel substrate.

For sample K2, the surface of samples K2-D was partially blistered, with areas where the paint was peeling and debris appearing in the grooves created when painting the sample with a brush. The more uniform painted areas still retain protection and good adhesion to the steel substrate. On the other side K2-I, the results are similar to those of sample K1-I.

Meanwhile, the G-0.05 paint sample was torched to 730 °C (the highest temperature when torched with gas) and maintained at this temperature for 30 min; the sample surface was not destroyed (as seen in Figure 6). The results show that

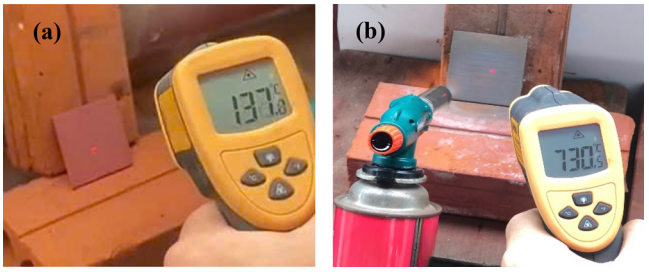

Figure 6. Paint samples G-0.05 were heated with shock (a) when the surface sample reached 137 °C and (b) after 30 min reached the highest temperatures of 730 °C.

https://doi.org/10.1021/acsomega.4c07850
ACS Omega 2025, 10, 5503−5516

the G-0.05 paint has superior thermal shock resistance compared to the K paint sample. This confirms that adding Graphene to the paint layer at a reasonable concentration (0.05%) will help increase the ability to The heat resistance of the paint increases significantly.

The detailed TGA/DTA data (Table 1) reveal that graphene enhances the thermal resistance of the coatings by delaying the onset of thermal degradation. This is attributed to the high thermal conductivity and barrier properties of graphene, which reduce heat transfer and structural breakdown within the silicate matrix. Among all samples, G-0.05 achieves the best performance, maintaining stability up to 798 °C. However, at higher graphene concentrations (G-0.1 and G-0.2), the benefits are offset by agglomeration, leading to minor early degradation.

Table 1. Table of Thermal Analysis Results (TGA/DTA)

sample	onset degradation temperature (°C)	temperature range of stability (°C)	maximum stability temperature (°C)
K (control)	~450	450–760	760
G-0.01	~480	480–774	774
G-0.02	~490	490–787	787
G-0.05	~500	500–798	798
G-0.1	~490	490–785	785
G-0.2	~490	490–785	785

2.2. Effect of Graphene on the Corrosion Resistance of the Inorganic Polymer Paint. The study was conducted on samples that were uncoated and coated with different concentrations of G by using electrochemical impedance spectroscopy and polarization curves.

2.2.1. Effect of Time on the Corrosion Resistance of the Studied Samples. The electrochemical impedance spectra of the samples over time immersed in a 3.5% NaCl solution are shown in Figure 7 (for the uncoated sample - control sample) and Figure 8 (for the samples coated with different concentrations of graphene).

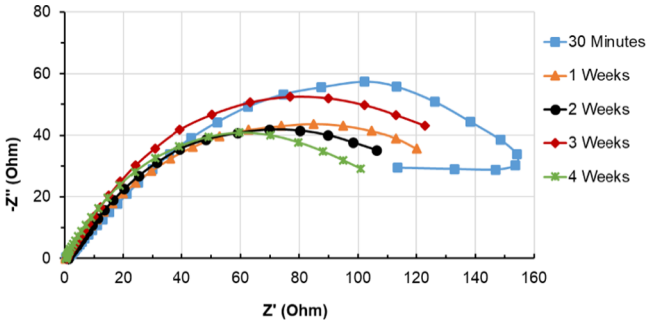

Figure 7. Nyquist plots of the control sample over time immersed in a 3.5% NaCl solution.

From Figure 7, in general, the impedance spectra of the uncoated steel samples consist of a single semicircle, indicating the kinetics of the corrosion process of steel. The larger the diameter of the semicircle, the greater the polarization resistance, meaning that the substrate corrodes at a slower rate. As the immersion time increases, the size of the semicircle decreases. This means that the corrosion resistance of the samples gradually decreases over time. Furthermore, when comparing the size of the semicircles in Figures 7 and 8, it shows that the control sample has the smallest semicircle among all the samples studied and is much smaller compared to the coated samples. This indicates the highest corrosion rate for uncoated steel. This is because, at the start of immersion, the solution directly contacts the steel surface, leading to rapid corrosion.

2.2.2. Effect of Graphene Concentration on the Corrosion Resistance. The results of the electrochemical impedance spectra of the steel samples, both uncoated and coated with different concentrations of graphene, at the same immersion times of 30 min, 1, 2, 3, and 4 weeks are presented in Figure 9.

At the 30 min immersion time: The samples are newly immersed in the corrosive environment and are not yet stable; therefore, the order of the spectra does not follow the same pattern as seen with longer immersion times. After 1 and 2 weeks of immersion time: In general, the impedance of the K, G 0.01, G 0.02, and G 0.05 samples is high, and there is no significant difference in the size of the impedance semicircles. After 3 and 4 weeks of immersion: the spectra show more distinct differences. The impedance spectrum of sample G-0.05 is the largest among all samples, followed by that of sample G-0.01. There are two samples in which the size of the impedance semicircle significantly decreases, indicating a sharp decline in corrosion resistance: sample K and sample G-0.02.

The impedance spectrum of the painted steel at different immersion times (Figures 8 and 9) all has the form of a nearly vertical line, proving that the coating is insulated from the substrate and the coating surface may have defects, which is not ideal, so the coating acts as a nonideal capacitor (Constant phase elements, Q). Constant phase elements represent nonideal or "leaky" capacitors. The nonideality of constant phase elements has been attributed to electrode surface heterogeneities occurring on the atomic scale, inhomogeneity of barrier film properties, and nonuniform distributions of potential and current.[22] As the immersion time increases, the size of the semicircle decreases and the impedance reaches its lowest value after 4 weeks of immersion. However, for the coating with 0.05% graphene, the semicircle size (impedance) at all immersion times is the largest among the coatings with different graphene concentrations.

The coating protects against the corrosion of metals by isolating the metal from the corrosive environment containing corrosive agents. Therefore, the ideal coating must be completely insulated (without defects) and contain no compounds that can react with the electrolyte solution. The coating acts as a pure capacitor, characterized by the capacitance of the coating. The equivalent circuit diagram consists of a resistance of the solution connected in series with a capacitor.[22] In this study, equivalent electrical circuits were used to model the impedance spectra of uncoated and coated inorganic polymer on steel substrate (Figure 10) with various parameters representing features like Solution resistance (R_s), Constant phase elements of the double layer (Q_{dl}), Constant phase elements of coating (Q_{coat}), and Charge-transfer resistance (R_{ct}). The CPE impedance is described by the following equation:

$$Z_{CPE} = 1/Y_0(J\omega)^n \quad (1)$$

where ω is the frequency and Y_0 is the capacitance of the system. For a constant phase element, the exponent n is less than one.[22] Typically, n is close to 1, representing a capacitive characteristic of the interfaces.

https://doi.org/10.1021/acsomega.4c07850
ACS Omega 2025, 10, 5503−5516

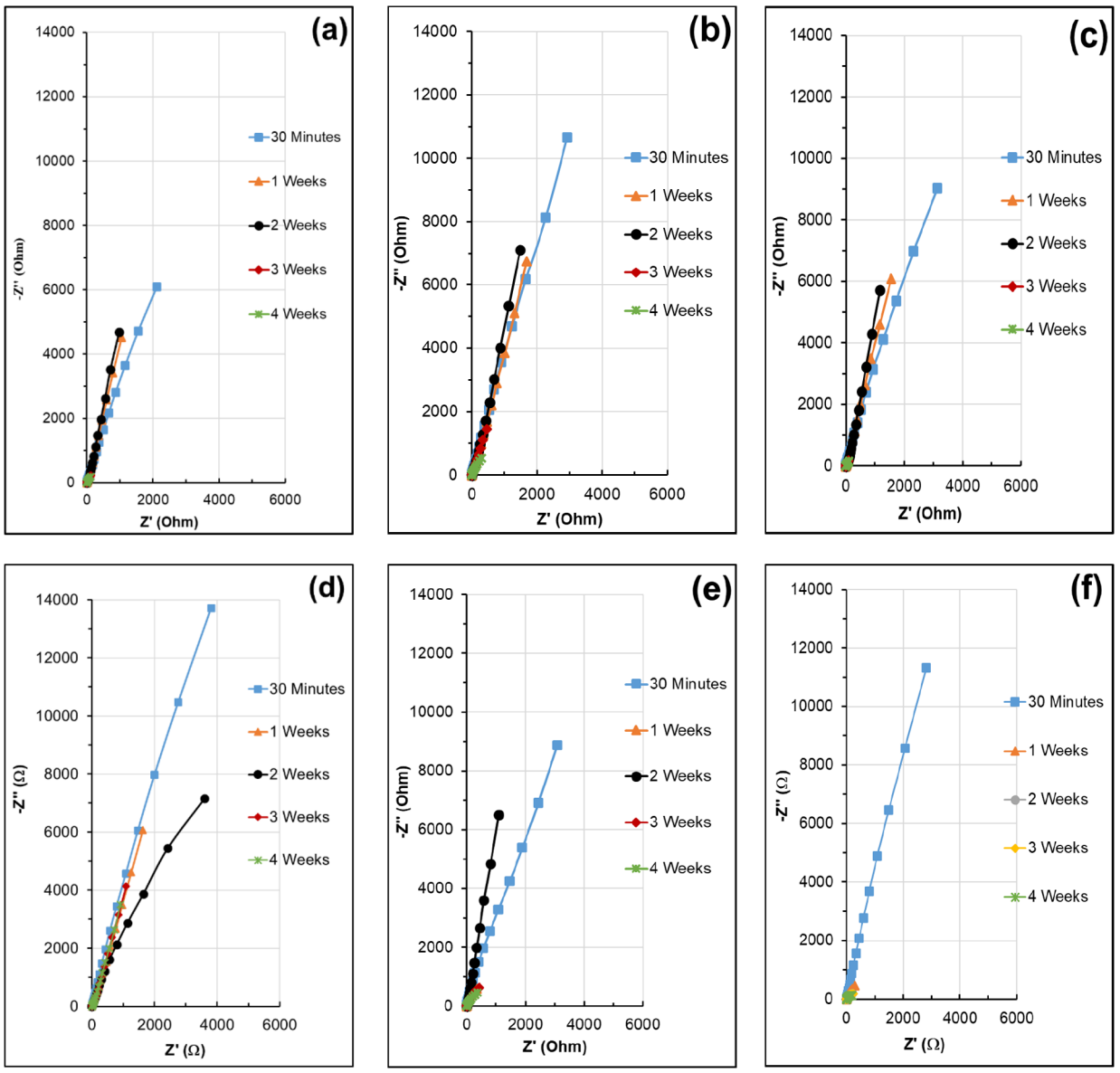

Figure 8. Nyquist plots of the samples over time: (a) Sample K; (b) Sample G-0.01; (c) Sample G-0.02; (d) Sample G-0.05; (e) Sample G-0.1; (f) Sample G-0.2 immersed in 3.5% NaCl solution.

Fitting results for uncoated steel sample (a) and for coated steel sample (b) after 1 week of immersion time in 3.5% NaCl solution with equivalent electrical circuits (Figure 10) are presented in Figure 11.

The EIS spectrum fitting results (Table 2) indicate that the solution resistance is very small (around 0.2−1.3 Ω), demonstrating that the 3.5% NaCl solution has good electrical conductivity. The charge transfer resistance (R_{ct}) of the uncoated steel decreases from 177 to 120 Ω as the immersion time increases from 30 min to 4 weeks. This decrease in R_{ct} with longer immersion times indicates the progressive corrosion of the steel over time.

For the painted sample, the film resistance is considered infinitely large, as the equivalent circuit consists of a resistor (R) in series with a constant phase element (Q), as analyzed earlier (Figure 10b). A larger CPE exponent n results in a more vertical spectrum, suggesting a higher film resistance. According to Table 2, the painted sample containing 0.05% graphene exhibits the largest n value across all test durations. Furthermore, n generally decreases with an increased immersion time in the 3.5% NaCl solution. This suggests that over time the paint layer absorbs the solution. However, even after 4 weeks, the painted sample continues to provide effective protection for the substrate.

Incorporating graphene into the coating at different concentrations also affects the corrosion resistance of the coating. However, the amount of graphene added to the coating needs to be appropriate to achieve good corrosion resistance. Adding a high concentration of graphene to the coating can reduce its corrosion resistance. This may be due to the high concentration of graphene tending to agglomerate in the coating, forming defects on the surface of the sample.[23,24] When the coating contains 0.05% graphene, it shows the best improvement in corrosion resistance.

The polarization curves of the steel samples, both uncoated and coated with different concentrations of graphene, after 4 weeks of immersion in 3.5% NaCl are shown in Figure 12. Figure 12 indicates that the corrosion potential of all samples

https://doi.org/10.1021/acsomega.4c07850
ACS Omega 2025, 10, 5503−5516

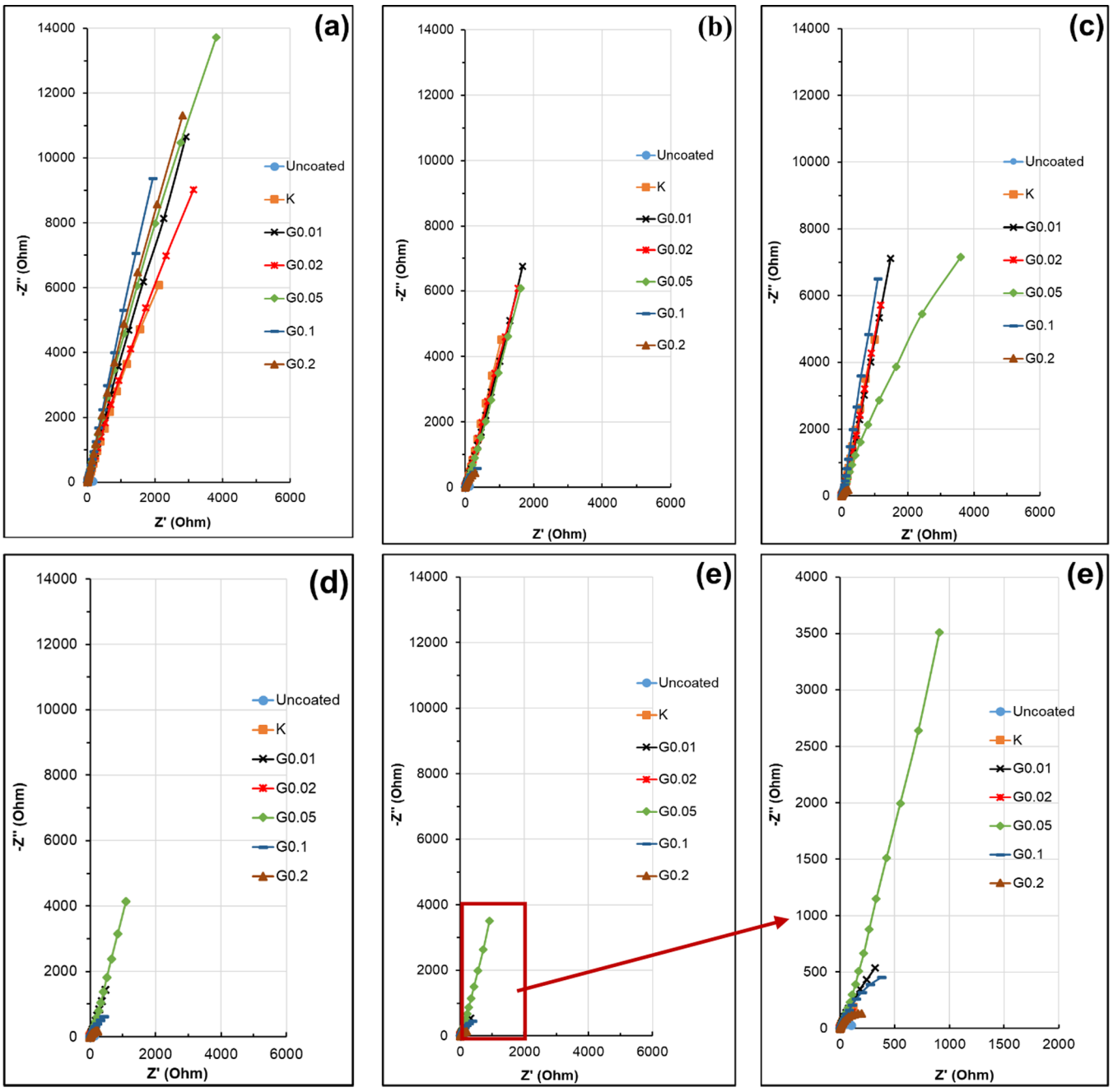

Figure 9. Nyquist plots of the samples over time: (a) 30 min; (b) 1 week; (c) 2 weeks; (d) 3 weeks; and (e) 4 weeks immersed in 3.5% NaCl solution.

does not change significantly when coated and when the coating includes different concentrations of graphene. However, when the samples are coated, both the anodic and cathodic branches of the polarization curves shift toward lower current densities. This indicates that the coating reduces the corrosion rate of the steel. Using the Tafel extrapolation method from the polarization curves, the corrosion parameters of the studied samples are presented in Table 3.

The results indicate that the uncoated steel substrate (control sample) suffers the most severe corrosion with the highest corrosion current density (19.58 μA/cm^2). Coating the steel substrate significantly reduces the corrosion current density. For the K coating (coating without graphene), the corrosion rate is higher compared to the samples with graphene concentrations ranging from 0.01% to 0.1%wt. The coating with 0.05% graphene showed the lowest corrosion rate (2.03 μA/cm^2). When the coating contains 0.2% graphene, the corrosion rate is higher than when there is no graphene. This may be due to the graphene agglomerating or being unevenly dispersed in the coating, creating defects on the coating surface, thus reducing the corrosion resistance of the coating. These results are consistent with several previous studies on the effect of graphene on the corrosion resistance of coatings.[23,24]

Additionally, the protective efficiency of the coating for the steel substrate (H_i) is calculated according to formula 2:

https://doi.org/10.1021/acsomega.4c07850
ACS Omega 2025, 10, 5503−5516

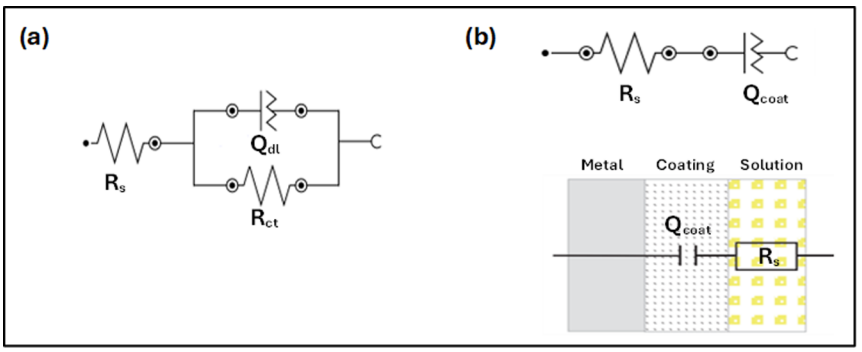

Figure 10. Equivalent electrical circuits used to analyze the EIS plots: (a) uncoated steel and (b) inorganic polymer paint coating on steel substrate with different graphene concentrations.[22]

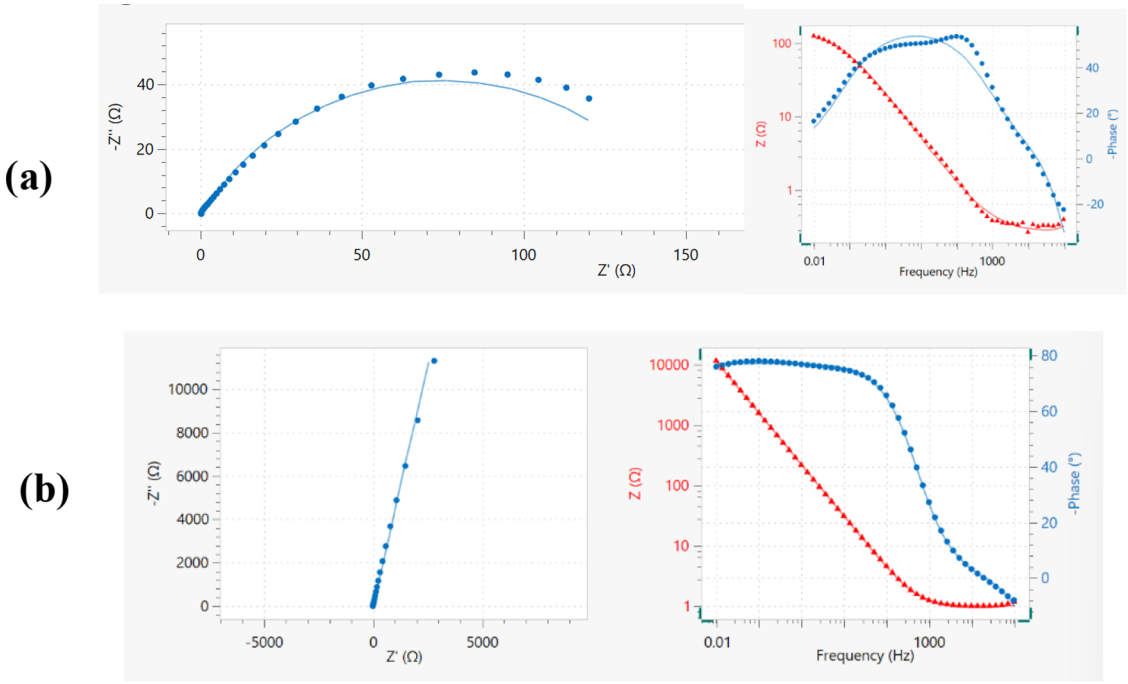

Figure 11. Fitting result for uncoated steel sample (a) and for coated steel sample (b) after 1 week of immersion time in 3.5% NaCl solution with equivalent electrical circuits Figure 10.

Table 2. Fitted Electrochemical Parameters of EIS of the Uncoated and Coated Samples

time	sample	R_s (Ω)	CPE−Y_0 × 10^{-3} (F s^{n-1})	n	R_{ct} (Ω)	time	sample	R_s (Ω)	CPE−Y_0 × 10^{-3} (F s^{n-1})	n	R_{ct} (Ω)
30 min	uncoated	0.224	2.98	0.71	177	1 week	uncoated	0.271	13.52	0.65	149
	K	0.458	1.43	0.81			K	0.569	2.101	0.78	
	G0.01	0.469	0.909	0.85			G0.01	0.859	1.409	0.82	
	G0.02	0.318	1.007	0.84			G0.02	1.269	1.756	0.79	
	G0.05	0.729	0.753	0.87			G0.05	0.969	1.496	0.82	
	G0.1	0.696	1.174	0.85			G0.1	0.745	13.65	0.79	
	G0.2	0.999	0.932	0.86			G0.2	0.495	15.47	0.71	
2 weeks	uncoated	1.131	32.7	0.67	144	4 weeks	uncoated	1.045	16.96	0.76	120
	K	1.162	2.101	0.79			K	0.322	33.6	0.73	
	G0.01	0.255	1.137	0.83			G0.01	0.394	13.11	0.77	
	G0.02	0.239	1.660	0.79			G0.02	0.248	35.58	0.69	
	G0.05	0.625	1.423	0.84			G0.05	0.272	2.502	0.79	
	G0.1	0.928	1.700	0.84			G0.1	0.284	12.68	0.75	
	G0.2	0.391	24.9	0.74			G0.2	0.104	25.11	0.75	

$$H_i = \frac{(i^0 - i)}{i^0} \times 100\% \quad (2)$$

where i^0 and i are the corrosion current densities of the uncoated steel substrate (control sample) and the coated steel samples, respectively, in $\mu A/cm^2$.

https://doi.org/10.1021/acsomega.4c07850
ACS Omega 2025, 10, 5503−5516

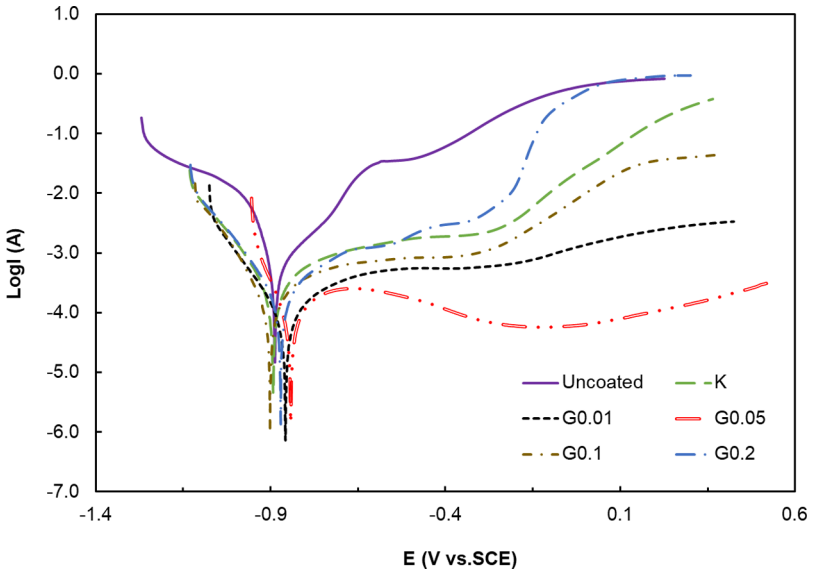

Figure 12. Polarization curves of the samples after 4 weeks of immersion in 3.5% NaCl.

Table 3. Tafel Extrapolation Results from the Polarization Curves of the Coated Samples after 4 Weeks of Immersion in 3.5% NaCl Solution

sample	E_c (-mV vs SCE)	i_c (μA/cm^2)	p (mm/year)	R_p (Ω)	H_i (%)
uncoated	883	19.58	0.227	39.672	
K	890	5.99	0.070	169.38	69.43
G0.01	851	2.48	0.029	454.85	87.35
G0.05	840	2.03	0.024	364.71	89.65
G0.1	900	4.73	0.055	238.63	75.82
G0.2	871	7.08	0.082	160.54	63.85

The calculated results, as presented in Table 3, show that the protective efficiency of the inorganic polymer coating for steel after 4 weeks of testing still ranges from approximately 64 to 90%. Generally, the graphene-containing coatings demonstrate better protection for the steel substrate compared to the coatings without graphene, except for the sample with a 0.2% graphene content. The highest protective efficiency for the steel substrate reaches 90% for the coating containing 0.05% graphene (increasing by around 20% compared to that of the paint without graphene). The presence of graphene in the coating consistently reduces the metal corrosion rate significantly, similar to experimental results of previous publications. Graphene's effectiveness in corrosion inhibition stems from its unique properties, including its impermeability, which blocks the penetration of corrosive agents such as water and oxygen, and its excellent electrical conductivity, which helps distribute electrochemical potential evenly, reducing localized corrosion.[23,24]

Thus, through studies on heat resistance and corrosion resistance of inorganic polymer coatings with and without graphene at different concentrations, the sample with 0.05% graphene exhibits the best heat resistance and corrosion resistance among the investigated coatings.

2.3. Influence of Graphene on the Surface Morphology and Structure of Inorganic Polymer Coating.

2.3.1. The Surface Morphology of Inorganic Polymer Coating by SEM/FESEM Images. SEM images of the coating samples at a magnification of 2000× are provided in Figure 13. The SEM images show that, overall, all three samples have relatively uniform surfaces. However, for the K coating sample, the largest particle size and a more porous surface are observed compared to the G0.05 and G0.1 coatings. A more porous surface allows the corrosive environment to penetrate through the coating more easily, resulting in a lower protective capability of the coating. Therefore, it can be observed that the surface morphology of G0.05 and G0.1 coatings is superior to that of the K coating.

Moreover, thin flakes appear on the surface of the G0.05 and G0.1 coatings, with sizes of approximately 10 μm, which may indicate the presence of graphene in the coating composition. The flake-shaped particles in the G0.05 coating are smaller and

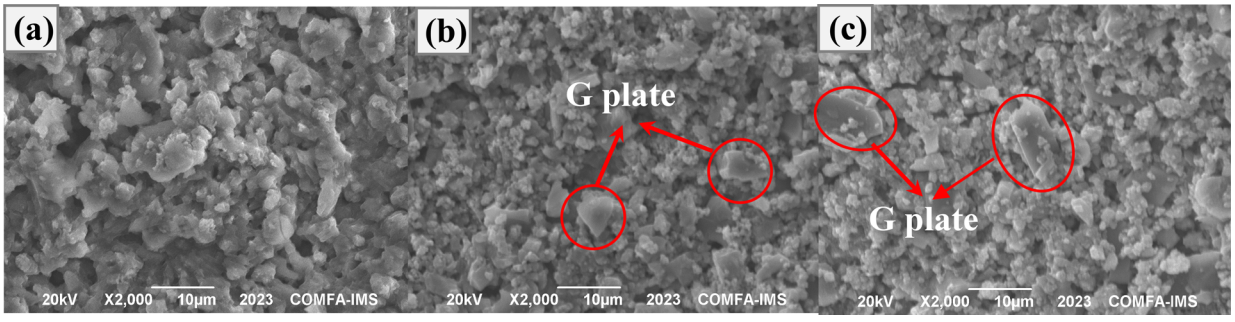

Figure 13. SEM images of the samples at 2000× magnification: (a) Sample K; (b) Sample G-0.05 and (c) Sample G-0.1.

https://doi.org/10.1021/acsomega.4c07850
ACS Omega 2025, 10, 5503−5516

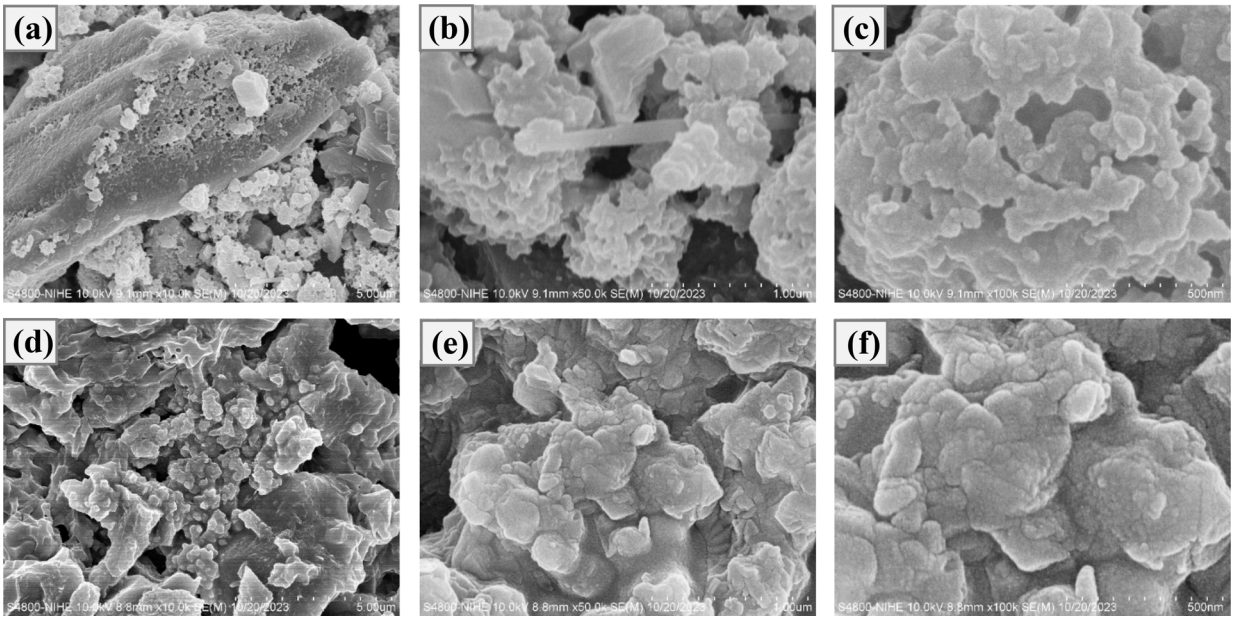

Figure 14. FESEM images of the K samples (a−c) and G-0.05 (d−f) at different magnifications.

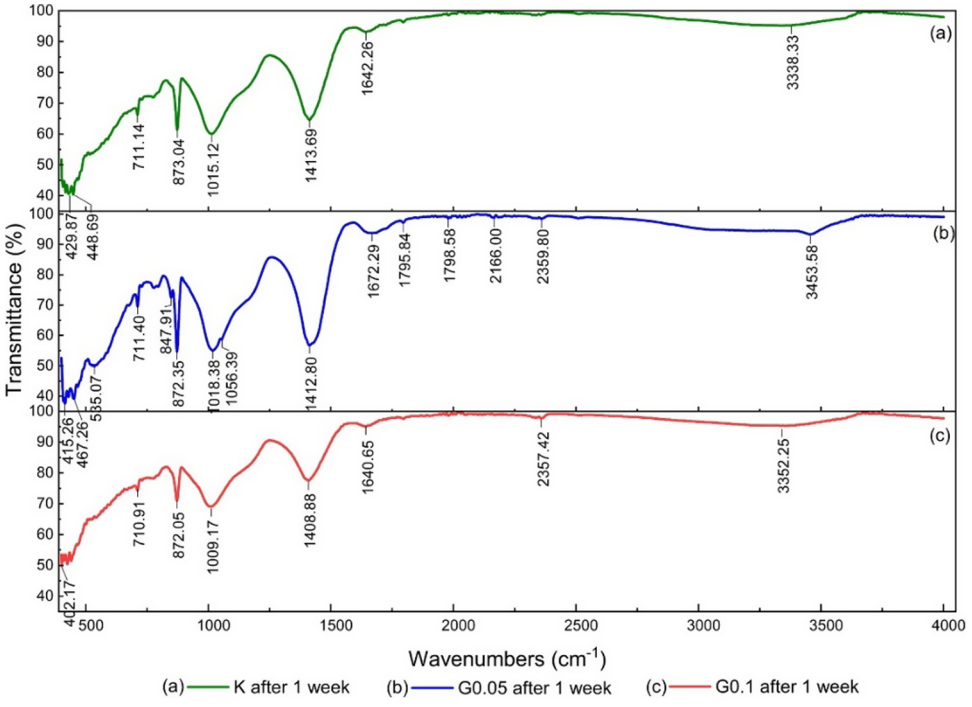

Figure 15. FTIR spectra of the three samples after 1 week.

more evenly distributed. This suggests that the dispersion of graphene at a concentration of 0.05% is better than that at 0.1%.

The results obtained from the FESEM method are entirely consistent with the studies on heat resistance and corrosion resistance of the coating samples, as presented earlier.

In Figure 14, when magnified at 100,000 times, it is evident that the K coating has a more porous surface with more voids compared to the G0.05 coating. The surface of the G0.05 coating is denser, indicating tighter bonds likely due to the presence of graphene in the coating composition. This results in longer, more continuous, and stronger polymer chains.

2.3.2. FTIR Analysis and Confirmation of Graphene Integration. From the FT-IR spectra (Figures 15 and 16), we can easily observe that there are no significant changes between the samples after 1 and 3 weeks. Except for the G-0.05 sample, a clear coalescence of peaks can be observed in the range of 1398.09−1412.8 cm^{-1} and 2965−3453 cm^{-1},[25−27] which may be attributed to the stretching of the C−OH group and the stretching of O−H present in graphene. However, these peaks are not evident in the G-0.1 sample after 1 and 3 weeks. This suggests that the G-0.05 sample significantly influences the properties of the material more than G-0.1. The characteristic signals of graphene, such as the stretching of C−O, C═O at 1720 cm^{-1} (carboxyl),[27−29] the bending of C═C

https://doi.org/10.1021/acsomega.4c07850
ACS Omega 2025, 10, 5503−5516

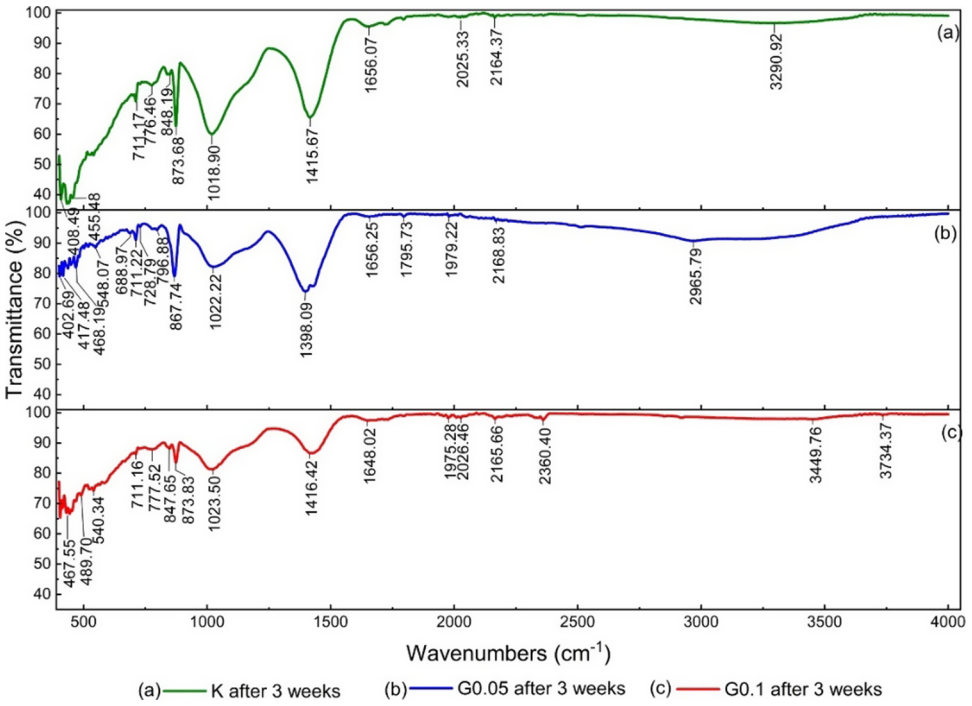

Figure 16. FTIR spectra of the three samples after 3 weeks.

Table 4. Physical Properties of the K Coating and G-0.05 Coating

no.	test criteria	unit	result for K coating	result for G-0.05 coating	test method
1	density	g/cm^3	1.66	1.66	TCVN 10237-1:2013
2	fineness	μm	25	20	TCVN 2091:2015
3	coverage	g/cm^2	167	142	TCVN 2095:1993
4	hardness		0.32	0.36	TCVN 2098:2007
5	surface drying time	h	0 h 35'	0 h 40'	TCVN 2096:2015
6	adhesion (Coating durability according to the grid-cut test)	type	0	0	TCVN 2097:2015
7	paint film thickness	μm	185	182	TCVN 9760:2013
8	heat resistance at 650 °C for 2 h	visual		no blistering, cracking, swelling	ASTM D 2485-18
	adhesion (coating durability according to the grid-cut test)	type	1	1	TCVN 2097:2015

at 1648 cm^{-1}, and the stretching vibration of C−O at 1023 cm^{-1},[19,25,27] also appear in the spectra of the graphene samples. This indicates that graphene has been incorporated and forms good bonds with the components in the coating.

FTIR spectroscopy was used to confirm the successful incorporation of graphene into the silicate-based paint matrix. The spectral data for the control sample (K) and graphene-enhanced samples (G-0.05 and G-0.1) were analyzed to identify functional groups and chemical interactions that signify the presence of graphene. Key observations are as follows.

2.3.2.1. Characteristic Peaks of Graphene. The presence of graphene in the paint matrix is indicated by several distinct peaks: **O−H Stretching (3000−3500 cm^{-1})**: A broad peak observed in graphene-containing samples corresponds to the stretching vibrations of hydroxyl groups (O−H) present on the graphene surface or edges, suggesting interactions with the silicate binder. **C═O Stretching (∼1720 cm^{-1})**: This peak, attributed to carbonyl groups, is weakly present in the G-0.05 and G-0.1 samples, indicating some oxidation of graphene, which enhances compatibility with the silicate matrix. **C═C Stretching (∼1640 cm^{-1})**: A prominent peak corresponds to the stretching of the sp^2 carbon network in graphene, confirming its structural integrity within the matrix.

2.3.2.2. Changes in Silicate Peaks. In the graphene-enhanced samples, minor shifts and intensity changes in the peaks related to the silicate binder were observed: **Si−O−Si Stretching (1000−1200 cm^{-1})**: A slight shift in this peak suggests an interaction between graphene and the silicate network, possibly through hydrogen bonding or van der Waals forces. **Si−O Stretching (400−800 cm^{-1})**: Enhanced intensity in this region indicates the improved structural stability of the paint due to graphene's reinforcing effect.

2.4. Influence of Graphene on Some Other Physicochemical Properties. In addition, properties such as heat resistance, corrosion resistance, surface morphology, and certain mechanical properties of the paint were also evaluated by the Institute of Building Materials according to ASTM and current Vietnamese Standards (TCVN). The results are presented in Table 4.

The results in Table 4 show that the fineness of sample G paint is smaller than that of sample K paint (decreasing from 25 to 20 μm when graphene is added to the paint). This finding is consistent with the study of painting the surface morphology through SEM and FESEM images. Additionally, when the samples were heated at 650 °C for 2 h, the surfaces of both K and G paints did not exhibit peeling, cracking, or blistering. The adhesion of the samples, determined according

https://doi.org/10.1021/acsomega.4c07850
ACS Omega 2025, 10, 5503−5516

to the grid-cut test before heating, was classified as grade 0, and after heating it was classified as grade 1. Although the adhesion decreased compared to that before heating, it still met the requirements for good adhesion of the coating to the metal substrate. Furthermore, the hardness of the paint increased from 0.32 to 0.36, indicating an improvement in the durability of the paint layer with the addition of graphene. However, the drying time of this paint also increased from 35 to 40 min, as graphene forms a tight network that retains the solvent in the paint longer, reducing the drying speed but enhancing adhesion. The coverage and specific gravity of G-0.05 paint are also lower compared to those of K paint, indicating better dispersion of the paint. These improvements suggest that graphene not only enhances the quality of the paint but also can adapt well to the specific requirements of various paint applications.

3. CONCLUSIONS

This study demonstrated the effects of incorporating graphene into inorganic polymer paints at varying concentrations (0, 0.01, 0.02, 0.05, 0.1, and 0.2% by weight) and evaluated its impact on key properties, such as thermal resistance, corrosion resistance, and surface morphology. The findings provided valuable insights into optimizing graphene-enhanced silicate coatings, with the main conclusions summarized as follows.

3.1. Optimal Graphene Concentration. Among all tested concentrations, 0.05% graphene was identified as the optimal concentration, significantly improving the overall performance of the paint. Excessive graphene content (>0.05%) resulted in agglomeration and surface defects, reducing the paint's effectiveness.

3.2. Enhanced Thermal Resistance. The incorporation of graphene increased the paint's thermal resistance, allowing it to withstand temperatures up to 798 °C, a 5% improvement compared to the graphene-free control sample. This enhancement is attributed to graphene's unique barrier properties and its interaction with the silicate matrix.

3.3. Improved Corrosion Resistance. Electrochemical analysis showed that graphene-enhanced paint exhibited approximately 20% higher corrosion resistance compared to the control sample. Nyquist plots and polarization curves confirmed that the coating containing 0.05% graphene achieved the highest impedance and lowest corrosion rate, indicating superior protection.

3.4. Improved Surface Morphology and Mechanical Properties. SEM and FESEM imaging revealed that the addition of graphene improved the surface smoothness, reduced porosity, and increased adhesion strength. These improvements were further supported by FTIR analysis, confirming the successful integration of graphene into the coating.

3.5. Practical and Environmental Significance. The graphene-enhanced silicate coating retained the environmental benefits of traditional silicate paints, such as low volatile organic compound (VOC) emissions and nonflammability, while providing superior performance. These characteristics make it a promising coating for industrial applications in high-temperature and corrosive environments.

3.6. Suggestions for Future Research.

- Explore advanced graphene dispersion techniques, such as chemical functionalization and tailored dispersants.
- Develop hybrid coatings by combining graphene with other nanomaterials to enhance properties.
- Conduct durability tests under harsh conditions like UV exposure and thermal cycling.
- Perform cost-benefit analyses for large-scale graphene-enhanced coatings production.
- Investigate applications of graphene coatings on concrete and ceramics to expand their versatility.

4. MATERIALS AND METHODS

4.1. Sample Preparation. The selection of graphene concentrations (0, 0.01, 0.02, 0.05, 0.1, and 0.2% by weight) was based on several factors derived from prior research and the unique characteristics of graphene as a nanomaterial.

Graphene has a high surface area and strong barrier properties, making it highly effective, even at low concentrations. Previous studies on graphene-based coating have shown significant improvements in thermal and corrosion resistance at concentrations below 1% by weight.[1−5] The range starts at 0.01% to evaluate the initial impact of graphene and determine the minimal effective concentration. Graphene tends to agglomerate at higher concentrations, leading to surface defects and reduced coating performance.[3,6] The upper limit of 0.2% was chosen to investigate whether there exists a critical threshold where dispersion challenges outweigh performance benefits. While extensive studies exist on organic and composite coatings using graphene, research on inorganic polymer systems is limited. The range from 0.01 to 0.2% ensures a comprehensive evaluation of graphene's effects on these coatings, helping to identify the optimal concentration specific to silicate-based systems.[6,11,17]

Preliminary trials conducted by the authors showed that graphene concentrations above 0.2% resulted in significant agglomeration, leading to uneven coatings and defects. Conversely, concentrations below 0.01% exhibited negligible improvements in thermal and corrosion resistance. Therefore, the selected range balances the practicality and experimental relevance. The graphene used in the research is a 4% solution purchased from VNGRAPHENE - Applied Nano Technology Joint Stock Company (ANTECH., Jsc, Vietnam), with a bulk density of 0.02−0.03 (g/mL), a diameter of 10−20 (μm), a thickness less than 15 (nm) and the content at least 98%. The graphene solution was dispersed in the inorganic polymer for 30 min by a magnetic stirring machine before being mixed with the dry composition (Figure 17). Graphene was included in the paint with different concentrations from 0 to 0.2% by weight, as shown in Table 5.

The inorganic polymer paint was produced with the process and components of silicate coating according to the document.[14] Research on the heat resistance of the coating was carried out by applying paint samples to a steel plate measuring 50 mm × 50 mm and 3 mm thick. To determine the corrosion resistance of the coating, a steel plate measuring 70 mm × 70 mm and 0.5 mm thick was used for electrochemical measurements. Before painting, the steel surface was cleaned by carefully polishing it with sandpapers ranging from 100 to 800 grade, followed by degreasing with soap, rinsing in distilled water, and drying on ethanol-impregnated plotting paper. For the electrochemical measurements, the samples were attached to 60 mm diameter and 70 mm high plastic tubes using two-component epoxy glue to contain the test solution (3.5% NaCl solution). The surface area used for the EIS test is 25.5 cm^2

https://doi.org/10.1021/acsomega.4c07850
ACS Omega 2025, 10, 5503−5516

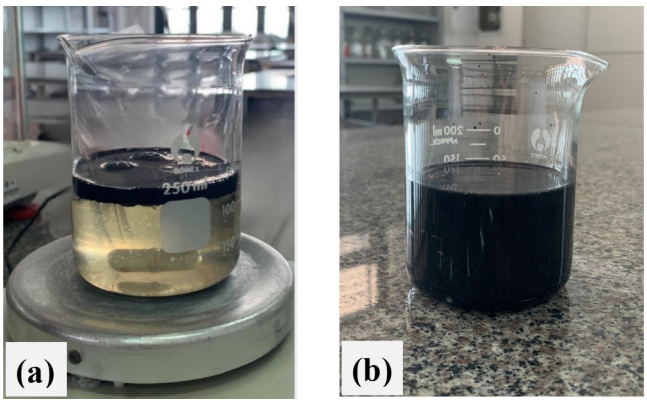

Figure 17. Graphene before and after dispersed in the inorganic polymer by magnetic stirring machine: (a) graphene before dispersed in the inorganic polymer, (b) graphene after dispersing for 30 min in the inorganic polymer.

Table 5. Paint Sample Symbols and Graphene Composition in the Paint (%G)

sample paint	K	G-0.01	G-0.02	G-0.05	G-0.1	G-0.2
graphene (wt %)	0	0.01	0.02	0.05	0.1	0.2

(calculated based on the inner diameter of the tubes connected to the coated surface).

4.2. Methods. The heat resistance of the coating with and without Graphene was studied using methods such as the TGA/DTA thermal analysis method; forced heating with direct surface pulse heat and heat in the furnace.

Thermogravimetric analysis (TGA) and derivative thermogravimetry (DTA) were performed using SETARAM, France, in the temperature range from room temperature to 1000 °C, with a heating rate of 10 °C/min under a nitrogen gas flow of 50 mL min^{-1}.

The forced heating with direct surface pulse heat used a gas torch and an infrared temperature gun to measure the temperature of the sample during the heating process. Paint samples on steel substrates are heated until the sample is destroyed or the sample reaches its maximum temperature for 30 min.

The paint samples on steel were calcinated at different temperatures: 650, 750, and 800 °C using a heating equipment Nabertherm (Germany) with a heating rate of 5 °C/min. After reaching the required temperature, the sample was stored for 1 or 2 h and then allowed to cool slowly in the oven to room temperature.

The surface morphology of the painted samples was investigated using a scanning electron microscope (SEM, JEOL 6490, Jed 2300, Japan) and a field emission scanning electron microscope (FESEM, S4800-Hitachi).

The corrosion resistance of the coating in 3.5% NaCl solution was determined by measuring electrochemical impedance spectroscopy (EIS) and the Polarization curve. All of the electrochemical tests were conducted using Autolab PGSTAT 302N (Netherlands) with a conventional three-electrode cell, where a platinum mesh was the counter electrode, and the saturated calomel electrode (SCE) was the reference electrode.

Electrochemical impedance measurements were conducted at free corrosion potential with an amplitude of 10 mV at a frequency in the range of 10 kHz ÷ 10 mHz. The samples with and without painting were measured by EIS in the test solution at different immersed times for 30 min, 1, 2, 3, and 4 weeks. EIS spectrum analysis was performed using Nova 2.1 software. EIS analysis was performed in triplicate for each sample to ensure repeatability and reliability. The data obtained from the EIS tests demonstrated good repeatability with a standard deviation below 5% across measurements.

Polarization measurements were carried out at the potential in the range of −300 to +1000 mV versus opened circuit potential at a scanning rate of 5 mV/s with the samples after 4 weeks of immersion time. The parameters of the steel corrosion process such as E_c (corrosion potential); I_c (corrosion current); and R_p (polarization resistance)··· were determined by the Tafel extrapolation method with the steel sample when uncoated and coated with the different paints.

The effect of time on reaction products as well as the bond formation of components with inorganic polymers was studied by Fourier transform infrared spectroscopy (FTIR). The paint layers were analyzed after 7 and 21 days of painting. FTIR spectra were measured on the Nicolet iS20 FTIR spectrometer operated in the mid-IR range of 4000−400 cm^{-1}, with spectra obtained at a spectral resolution of 8 cm^{-1} in transmittance mode.

AUTHOR INFORMATION

Corresponding Author

Cuong Manh Le − *Hanoi University of Civil Engineering, Ha Noi 100000, Vietnam;* orcid.org/0000-0002-4550-7978; Email: cuonglm@huce.edu.vn

Authors

Huyen T. T. Bui − *Hanoi University of Civil Engineering, Ha Noi 100000, Vietnam;* orcid.org/0000-0002-0880-1924

Anh Nguyet Hoang − *Hanoi University of Civil Engineering, Ha Noi 100000, Vietnam*

Complete contact information is available at: https://pubs.acs.org/10.1021/acsomega.4c07850

Notes

The authors declare no competing financial interest.

ACKNOWLEDGMENTS

This research is funded by Hanoi University of Civil Engineering (HUCE) under grant number 27-2023/KHXD-TĐ.

REFERENCES

(1) Pan, C.; He, J.; Zhu, J.; Li, S.; Li, W.; Yang, W.; Li, W. Corrosion Control by Carbon-Based Nanomaterials: A Review. *ACS Applied Nano Materials* **2024**, *7* (3), 2515−2528.

(2) Amin, I.; Batyrev, E.; de Vooys, A.; van der Weijde, H.; Shiju, N. R. Covalent polymer functionalization of graphene/graphene oxide and its application as anticorrosion materials. *2D Materials* **2022**, *9* (3), No. 032002.

(3) Othman, N. H.; Che Ismail, M.; Mustapha, M.; Sallih, N.; Kee, K. E.; Ahmad Jaal, R. Graphene-based polymer nanocomposites as barrier coatings for corrosion protection. *Prog. Org. Coat.* **2019**, *135*, 82−99.

(4) Li, S.; Song, G.; Zhang, Y.; Fu, Q.; Pan, C. Graphene-Reinforced Zn−Ni Alloy Composite Coating on Iron Substrates by Pulsed Reverse Electrodeposition and Its High Corrosion Resistance. *ACS Omega* **2021**, *6* (21), 13728−13741.

(5) Afsharimani, N.; Durán, A.; Galusek, D.; Castro, Y. Hybrid Sol−Gel Silica Coatings Containing Graphene Nanosheets for Improving

https://doi.org/10.1021/acsomega.4c07850
ACS Omega 2025, 10, 5503−5516

the Corrosion Protection of AA2024-T3. *Nanomaterials* **2020**, *10* (6), 1050.
(6) Wang, C.; Wang, W.; Zhu, S.; Wang, F. Oxidation inhibition of γ-TiAl alloy at 900°C by inorganic silicate composite coatings. *Corros. Sci.* **2013**, *76*, 284−291.
(7) Hussain, A. K.; Sudin, I.; Basheer, U. M.; Yusop, M. Z. M. *A review on graphene-based polymer composite coatings for the corrosion protection of metals.* **2019**, *37* (4), 343−363.
(8) Huang, H.; Sheng, X.; Tian, Y.; Zhang, L.; Chen, Y.; Zhang, X. Two-Dimensional Nanomaterials for Anticorrosive Polymeric Coatings: A Review. *Ind. Eng. Chem. Res.* **2020**, *59* (35), 15424−15446.
(9) Rokaya, S.; Adhikari, S. *A brief overview of inorganic polymers and their applications*, 2022.
(10) Loganina, V. I.; Kislitsyna, S. N.; Mazhitov, Y. B. Development of sol-silicate composition for decoration of building walls. *Case Studies in Construction Materials* **2018**, *9*, No. e00173.
(11) Graphene inorganic paint and use method thereof. CN103275542A China, 2013.
(12) Dhanuk, K. *Inorganic polymers, Paints and lubricants in Mechanical Engineering*, 2023.
(13) Li, M.; Hong, Y.; Yu, H.; Qu, S.; Wang, P. A novel high solar reflective coating based on potassium silicate for track slab in high-speed railway. *Construction and Building Materials* **2019**, *225*, 900−908.
(14) Le, C. M.; Le, T.-H. The Study's Chemical Interaction of the Sodium Silicate Solution with Extender Pigments to Investigate High Heat Resistance Silicate Coating. *J. Anal. Methods Chem.* **2021**, *2021* (1), No. 5510193.
(15) Manh, C. L.; Minh, N. T. T.; Thi, L. A. L.; Xuan, K. B.; Hoang, T. N. Synthesis of inorganic polymer sodium aluminum silicate system based on sodium silicate and application as film forming agent for silicate paint. *Vietnam J. Catal. Adsorpt.* **2022**, *11* (4), 6−11.
(16) Le, M.-C.; Le, T.-H.; Bui Thi, T.-H.; Nguyen, Q.-D.; Do Thi, T.-H.; Tran Thi, M.-N. Synthesizing and Evaluating the Photocatalytic and Antibacterial Ability of TiO_2/SiO_2 Nanocomposite for Silicate Coating. *Front. Chem.* **2021**, *9*, No. 738969.
(17) Ansari, S. A. Graphene Quantum Dots: Novel Properties and Their Applications for Energy Storage Devices. *Nanomaterials* **2022**, *12* (21), 3814.
(18) Farooq, N.; Rehman, Z.; Hareem, A.; Masood, R.; Ashfaq, R.; Fatimah, I.; Hussain, S.; Ansari, S. A.; Parveen. Graphene Oxide and Based Materials: Synthesis, Properties, and Applications - A Comprehensive Review. *MatSci. Express* **2024**, *01* (04), 185−231.
(19) Kanta, U.-A.; Thongpool, V.; Sangkhun, W.; Wongyao, N.; Wootthikanokkhan, J. Preparations, Characterizations, and a Comparative Study on Photovoltaic Performance of Two Different Types of Graphene/TiO2 Nanocomposites Photoelectrodes. *J. Nanomater.* **2017**, *2017* (1), No. 2758294.
(20) Attia, N. F.; Elashery, S. E. A.; Zakria, A. M.; Eltaweil, A. S.; Oh, H. Recent advances in graphene sheets as new generation of flame retardant materials. *Materials Science and Engineering: B* **2021**, *274*, No. 115460.
(21) Attia, N. F.; Zakria, A. M.; Nour, M. A.; Abd El-Ghany, N. A.; Elashery, S. E. A. Rational strategy for construction of multifunctional coatings for achieving high fire safety, antibacterial, UV protection and electrical conductivity functions of textile fabrics. *Materials Today Sustainability* **2023**, *23*, No. 100450.
(22) Lazanas, A. C.; Prodromidis, M. I. Electrochemical Impedance Spectroscopy - A Tutorial. *ACS Measurement Science Au* **2023**, *3* (3), 162−193.
(23) Youh, M.-J.; Huang, Y.-R.; Peng, C.-H.; Lin, M.; Chen, T.-Y.; Chen, C.-Y.; Liu, Y.-M.; Pu, N.-W.; Liu, B.-Y.; Chou, C.-H.; Hou, K.-H.; Ger, M.-D. Using Graphene-Based Composite Materials to Boost Anti-Corrosion and Infrared-Stealth Performance of Epoxy Coatings. *Nanomaterials* **2021**, *11*, 1603.
(24) Salasel, A. R.; Bhowmick, S.; Riahi, R.; Alpas, A. T. Role of graphene concentration on electrochemical and tribological properties of graphene-poly(methyl methacrylate) composite coatings. *Journal of Composite Materials* **2023**, *57* (24), 3877−3896.
(25) Faniyi, I. O.; Fasakin, O.; Olofinjana, B.; Adekunle, A. S.; Oluwasusi, T. V.; Eleruja, M. A.; Ajayi, E. O. B. The comparative analyses of reduced graphene oxide (RGO) prepared via green, mild and chemical approaches. *SN Appl. Sci.* **2019**, *1* (10), 1181.
(26) Mehmood, A.; Mujawar, M. N.; Khalid, M.; Jagadish, P.; Walvekar, R.; Abdullah, E. C. Graphene/PVA buckypaper for strain sensing application. *Sci. Rep.* **2020**, *10* (1), 20106.
(27) Çiplak, Z.; Yildiz, N.; Çalimli, A. Investigation of Graphene/Ag Nanocomposites Synthesis Parameters for Two Different Synthesis Methods. *Fullerenes, Nanotubes Carbon Nanostruct.* **2014**, *23*, 361−370.
(28) Ibrahim, S.; Ahmad, A.; Mohamed, N. S. Characterization of Novel Castor Oil-Based Polyurethane Polymer Electrolytes. *Polymers* **2015**, *7*, 747−759.
(29) Aziz, M.; Halim, F.; Jaafar, J. Preparation and Characterization of Graphene Membrane Electrode Assembly. *J. Teknol.* **2014**, *69*, 11−14.

https://doi.org/10.1021/acsomega.4c07850
ACS Omega 2025, 10, 5503−5516